

Pre-print version

Final version is available through <https://doi.org/10.1109/ISGTEUROPE62998.2024.10863675>

A. Knockaert, L. Papangelis, P. Tielens and K. Karoui, "Supervisory control of Bipole-based Multi-Terminal HVDC grids using Model Predictive Control including asymmetric operation," 2024 IEEE PES Innovative Smart Grid Technologies Europe (ISGT EUROPE), Dubrovnik, Croatia, 2024, pp. 1-6, doi: 10.1109/ISGTEUROPE62998.2024.10863675.

Supervisory control of Bipole-based Multi-Terminal HVDC grids using Model Predictive Control including asymmetric operation

Antoine Knockaert

Tractebel

Brussels, Belgium

antoine.knockaert@engie.com

Lampros Papangelis

Tractebel

Brussels, Belgium

lampros.papangelis@engie.com

Pieter Tielens

Tractebel

Brussels, Belgium

pieter.tielens@engie.com

Karim Karoui

Tractebel

Brussels, Belgium

karim.karoui@engie.com

Abstract—Multi-Terminal DC (MTDC) grids are gaining attention as potential architectures to interconnect multiple AC areas and renewable energy production sites. While symmetric monopole configurations are currently the most common, increased power flow and reliability needs are increasing the interest towards bipole configuration with ground return or Dedicated Metallic Return (DMR). This paper presents a supervisory control scheme based on Model Predictive Control (MPC) that smoothly steers the MTDC grid between operating points while ensuring compliance with various system limits. At the heart of the MPC lies a constrained optimization problem that determines a series of actions to be taken to best meet the power and average voltage references. Additionally, this paper demonstrates the capability of the controller to keep between limits the DMR current and neutral voltages following the outage of a single pole.

Index Terms—HVDC, MPC, VSC, MTDC, Bipolar, DMR

I. INTRODUCTION

The integration of renewable energy sources and the growing electricity exchanges between areas has necessitated the development of innovative grid architectures and control strategies. MTDC grids are able to tackle both challenges while offering various advantages over their AC counterpart, such as higher transmission length without stability limitation, a higher controllability, no reactive losses, interconnection of asynchronous areas and lower losses, among others [1]

With most of the HVDC connections today being point-to-point links, MTDC grids still require appropriate control schemes to be developed [2]. This paper presents the implementation of a supervisory MPC-based scheme applied on bipolar MTDC grids. The goal is to control the power flows and average voltage of the grid based on reference setpoints received from an upper control level, while respecting various system constraints. To show the capabilities of such a controller, multiple simulation cases and their results will be discussed. Those cases include normal operation of the MTDC as well as faulty operation.

This work was funded by the Horizon Europe program through the project “HVDC-based Grid Architectures for Reliable and Resilient WideSpread Hybrid AC/DC Transmission Systems” (HVDC-WISE) (Grant ID: 101075424).

This paper is organized as follows: The proposed control method is described in section II. Next, the applied test system and software implementation are given in section III. section IV presents and further discusses the obtained simulation results. Finally, the main conclusions are drawn in section V.

II. PROPOSED CONTROL METHOD

A. Overview of HVDC grid control

Although practical experience with VSC-based MTDC systems in very limited, it is expected that they will be governed by a set of controls, with a hierarchical structure. The CEN-ELEC [3] guidelines have been proposed for MTDC grids, and are hereafter summarized.

1) *Core control functions*: The core control functions of the converters are relying on locally available information and measurements. These functions correspond to the critical operation of the converters (valve switching and internal converter controls) and of the HVDC grid (DC voltage control). They have very fast response times compared to other levels of control, down to some tens of milliseconds.

This paper does not focus on the core control functions, however the proposed scheme is directly linked with the DC voltage control. Therefore, it is hereafter briefed. The VSC converters of the MTDC grid are controlling their DC terminal voltage with the DC voltage droop method, for which several implementations can be found in the literature, e.g., [4] and [5]. In its simplest version, it defines a $P(V)$ characteristic for some of the VSCs in the HVDC grid. It is defined by a DC power setpoint P_{set} , a DC voltage setpoint V_{set} and a droop gain K_V . The relationship between the power of each VSC and the DC voltage is then given by (1):

$$P = P_{set} - K_V (V - V_{set}) \quad (1)$$

A positive value of P indicates that power is flowing into the HVDC system. The idea behind the droop control is inspired by the primary frequency control in AC systems: a change in the power injected in the MTDC network following an outage of a VSC or a change in production of the offshore wind farm will cause a change in the power balance of the grid.

Instantaneously, the DC capacitance of the network (i.e., DC cable and converter capacitance, if any) will cover the change, inducing a DC voltage variation and consequently the VSC power adjustment according to their droop characteristics.

2) *Supplementary control functions*: These functions concern the global DC grid control and the AC/DC grid control, with response times ranging from some seconds up to several minutes, hours or even longer. It is composed of the global DC grid control and the AC/DC grid control.

The global DC grid control has multiple functions as described in [3]. For instance, it continuously processes converter schedules received by the AC/DC grid control, while ensuring a secure steady state operation of the HVDC grid. Furthermore, it re-optimizes the DC network operation after unscheduled events and reacts on deviations from the scheduled power flows. This control concept, inspired by the work performed in [6], has been implemented with Model Predictive Control, technique hereafter discussed later in this section.

On the other hand, the AC/DC grid control level provides the power schedules to the coordinated DC grid control. Those can be obtained using for example a combined AC/DC SCOPF including AC and DC contingencies. This is not further discussed in this paper.

B. Overall control structure

The AC/DC grid control and the global DC grid control are closely interrelated and need to exchange information at regular intervals. The AC/DC grid controls focuses on the combined AC/DC system (which can involve more than one AC or HVDC grids) to ensure its optimal and secure operation. The tertiary and supervisory control denoted in Fig. 1 correspond to the AC/DC grid control and the HVDC control, respectively.

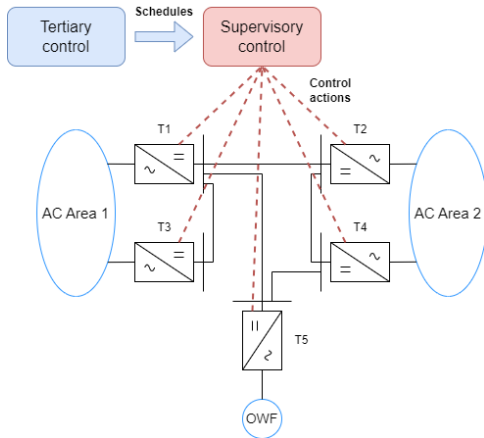


Fig. 1. Overview of the control structure

C. Global HVDC grid control

The control developed in this work is inspired from the work in [7], where the concept of MPC was used. Hence, the main objectives of this controller, as listed in [7], are preserved.

Fundamentally, the controller progressively drives the system from the current operating point to the desired one, while

preventing or correcting any voltage or current violations. It can accommodate the varying power injections by renewable sources and is robust to system inaccuracies as well as disturbances, such as outages of AC/DC converters or DC cables/lines. Through a smooth transition between operating points, it avoids excessive impact on the adjacent AC systems and facilitates the provision of additional services, such as frequency support. Finally, the controller avoids extensive communication requirements between controllers.

In addition to the capabilities presented above and described in [7], this work has extended the application of the MPC controller to bipolar systems in which it is able to redistribute the power among converters and poles and the regulation of the neutral currents in the DMR or ground return path in order to keep the neutral point voltages between pre-defined limits.

D. Brief description of MPC

MPC is a control algorithm used to control a process by ensuring that a set of constraints are respected during operation. Essentially, it computes a series of control actions to be taken in order to achieve a multi-step objective [8].

1) *Control formulation*: The objective of the MPC is to steer the VSCs of the HVDC system between operating points while ensuring that no system constraint is violated. Those constraints are listed here:

- Lower and upper limits on DC node voltages;
- Lower and upper limits on the power of each VSC;
- Limit on the rate of change of each VSC power;
- Upper limit on each DC branch current;
- Average DC voltage constraint;
- Upper limit on DMR or ground return currents;
- Upper limit on neutral DC node voltages.

In order to achieve the aforementioned goals, the controller gathers measurements of the HVDC grid at regular time intervals. Therefore, at time k , the following measurements are available to the supervisory controller: $\mathbf{P}_m^+(k)$ and $\mathbf{P}_m^-(k)$ i.e., the vectors including the VSC powers, $\mathbf{V}_m^+(k)$ and $\mathbf{V}_m^-(k)$ the vectors of pole-to-neutral DC node voltages and $\mathbf{I}_m^+(k)$ and $\mathbf{I}_m^-(k)$ the vectors of DC branch currents for the positive and negative pole respectively.

Based on these measurements, a reference trajectory is defined [9] bringing the VSC powers at each terminal to their reference values \mathbf{P}^{ref} , as provided by the AC/DC grid control for each VSC terminal (i.e. for both poles), in N_c control steps. This trajectory is linear and defined in (2).

$$\mathbf{P}^{\text{ref}}(k+j) = (\mathbf{P}_m^+(k) + \mathbf{P}_m^-(k)) + \frac{j}{N_c} [\mathbf{P}^{\text{ref}} - (\mathbf{P}_m^+(k) + \mathbf{P}_m^-(k))] \quad (2)$$

An illustration of the reference trajectory for a single converter and $N_c = 3$ is given in Fig. 2.

At this point, it is important to highlight the difference in the calculation of the power references between non-dispatchable and dispatchable terminals. The non-dispatchable terminals are injecting/exporting power from the MTDC grid as dictated by external factors (e.g., wind speed for offshore wind farms).

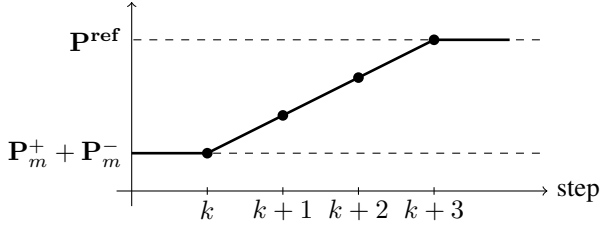


Fig. 2. Example of ref. trajectory for $N_c = 3$ for one terminal

Hence their power reference should be taken equal to their latest measured power.

At the core of the MPC scheme lies an optimization problem. It aims at minimizing the deviations of the predicted VSC power setpoints from the reference trajectory. Additionally, as a way to suggest to the MPC that it should prefer a balanced operating point when the MTDC grid is balanced, a second term integrating the DMR currents is added, as per (3):

$$\min \sum_{j=1}^{N_c} \left\| \mathbf{P}^{\text{ref}}(k+j) - (\mathbf{P}^+(k+j) + \mathbf{P}^-(k+j)) \right\|_{\mathbf{W}}^2 + \sum_{j=1}^{N_c} \left\| \mathbf{I}^0 \right\|_{\mathbf{W}_0}^2 \quad (3)$$

where \mathbf{W} is a diagonal weighting matrix assigned to the deviations of total VSC terminal power (i.e., the sum of both poles) from their references \mathbf{P}^{ref} . Bigger weight is assigned to the non-dispatchable terminals in order to modify their operation only when actions on the dispatchable VSCs are not sufficient. The weighting matrix \mathbf{W}_0 has a much smaller weight, and is used to direct the solution towards balanced operation points in balanced configurations.

The optimization problem is subject to a set of constraints. For the positive and negative poles at each step (for $j = 1, \dots, N_c$), (4) expresses the DC voltage constraint, (5) the VSC power constraint, (6) the branch power constraint, (7) the power variation constraint and (8) the DC average voltage constraint with $V_{\text{avg}}^{\text{ref}}$ the reference average voltage.

$$\mathbf{V}_{\min}^{\pm} \leq \mathbf{V}^{\pm}(k+j) \leq \mathbf{V}_{\max}^{\pm} \quad (4)$$

$$\mathbf{P}_{\min}^{\pm} \leq \mathbf{P}^{\pm}(k+j) \leq \mathbf{P}_{\max}^{\pm} \quad (5)$$

$$-\mathbf{I}_{\max}^{\pm} \leq \mathbf{I}^{\pm}(k+j) \leq \mathbf{I}_{\max}^{\pm} \quad (6)$$

$$\Delta \mathbf{P}_{\min}^{\pm} \leq \mathbf{P}^{\pm}(k+j) - \mathbf{P}^{\pm}(k+j-1) \leq \Delta \mathbf{P}_{\max}^{\pm} \quad (7)$$

$$\mathbf{V}_{\text{avg}}^{\pm}(k+j) = \mathbf{V}_{\text{avg}}^{\pm}(k) + \frac{j}{N_c} [V_{\text{avg}}^{\text{ref}} - \mathbf{V}_{\text{avg}}^{\pm}(k)] \quad (8)$$

For the return path currents \mathbf{I}^0 and DC neutral voltages \mathbf{V}^0 at each step (for $j = 1, \dots, N_c$), (9) expresses the neutral point voltage constraint and (10) the return path current constraint.

$$\mathbf{V}_{\min}^0 \leq \mathbf{V}^0(k+j) \leq \mathbf{V}_{\max}^0 \quad (9)$$

$$-\mathbf{I}_{\max}^0 \leq \mathbf{I}^0(k+j) \leq \mathbf{I}_{\max}^0 \quad (10)$$

Finally, in order for the optimization problem to evaluate the predicted evolution of the various variables due to the

sequential control actions $\Delta \mathbf{P}_{\text{set}}^{\pm}(k+j-1)$ for $j = 1, \dots, N_c$, equality constraints are included in the formulation. The DC voltage predictions are expressed by (11), the active powers by (12), the branch currents by (13), the neutral currents by (14) and the neutral voltages by (15).

$$\Delta \mathbf{P}_{\text{set}}^{\pm}(k+j-1) = \mathbf{S}_{\mathbf{P}}^{\pm} [\mathbf{V}^{\pm}(k+j) - \mathbf{V}^{\pm}(k+j-1)] \quad (11)$$

$$\Delta \mathbf{P}_{\text{set}}^{\pm}(k+j-1) = \mathbf{P}^{\pm}(k+j) - \mathbf{P}^{\pm}(k+j-1) + \mathbf{K}_{\mathbf{V}}^{\pm} [\mathbf{V}^{\pm}(k+j) - \mathbf{V}^{\pm}(k+j-1)] \quad (12)$$

$$\mathbf{I}^{\pm}(k+j) = \mathbf{I}^{\pm}(k+j-1) + \mathbf{S}_{\mathbf{I}}^{\pm} \Delta \mathbf{P}_{\text{set}}^{\pm}(k+j-1) \quad (13)$$

$$\mathbf{I}^0(k+j) = \mathbf{I}^+(k+j) - \mathbf{I}^-(k+j) \quad (14)$$

$$\mathbf{I}^0(k+j) = \mathbf{G}^0 \mathbf{V}^0(k+j) \quad (15)$$

2) *Tuning and response time*: The settling time of the system is directly linked to the control horizon as in [7]. This settling time can be calculated easily by neglecting the losses on the MTDC grid and assuming no current or voltage limit violations. Indeed, after one control step of the MPC the VSC powers is expressed by (16):

$$\mathbf{P}(k+1) = \mathbf{P}(k) + \frac{\mathbf{P}^{\text{ref}} - \mathbf{P}(k)}{N_c} \quad (16)$$

Hence, the error $\delta \mathbf{P}$ after one step can be expressed by (17):

$$\delta \mathbf{P}(k+1) = \mathbf{P}^{\text{ref}} - \mathbf{P}(k+1) = \frac{N_c - 1}{N_c} (\mathbf{P}^{\text{ref}} - \mathbf{P}(k)) \quad (17)$$

And more generally, the error at the n -th step:

$$\delta \mathbf{P}(k+n) = \left(\frac{N_c - 1}{N_c} \right)^n (\mathbf{P}^{\text{ref}} - \mathbf{P}(k)) \quad (18)$$

Within this paper, a step time of 5 s for a settling time of 40 s has been chosen. This corresponds to 8 control steps to obtain a desired 5% settling time, which through (18) translates to a maximum control horizon N_c of 3 steps as per (19).

$$\left(\frac{N_c - 1}{N_c} \right)^8 \leq 0.05 \Rightarrow N_c^{\text{max}} = 3 \text{ steps} \quad (19)$$

III. IMPLEMENTATION

A. Test system description

The proposed MPC is tested on the HVDC grid shown in Fig. 1. The HVDC grid is composed of 5 terminals interconnecting two AC areas and one offshore wind farm. Each terminal embeds two converters, and each connections adopts a bipole configuration with DMR. Note that only one pole is shown in Fig. 1. The neutral point of terminal T1 is selected as the grounding point.

The relevant parameters of the VSCs and the DC cables are given in Table I and Table II, respectively. The resistance of the DMR cables is assumed 120 % of the resistance of the corresponding pole cables.

The MPC parameters are as follows (with a base power of 100 MW and a base voltage of 525 kV). The active power limits for all VSCs are $P_{\min} = -P_{\max} = -10$ pu except the ones connected to terminal T5 for which the limits are $P_{\min} = -P_{\max} = -3.5$ pu. The DC current limits for all

TABLE I
VSC PARAMETERS (POSITIVE AND NEGATIVE POLES)

VSC name	Rating (MW)	K_V (MW/kV)	Dispatchable?
T1	1000	10	Yes
T2	1000	10	Yes
T3	1000	10	Yes
T4	1000	10	Yes
T5	350	0	No

TABLE II
DC CABLE PARAMETERS (POSITIVE AND NEGATIVE POLES)

Name	Rating (MW)	Resistance (Ω)
T1-T2	1000	1.5
T1-T3	1000	3.5
T1-T5	350	2.5
T2-T4	1000	4.0
T4-T5	350	1.5

branches are set to $I_{max} = 10$ pu except for the two branches connected to terminal T5, which have a lower capacity with $I_{max} = 3.5$ pu. The DC voltage limits are set to $V_{min} = 0.96$ pu and $V_{max} = 1.04$ pu. Finally, the rate of change of power limits are neglected by assigning them very high values.

The connected AC areas are modelled as infinite grids, as the focus is on the multi-terminal HVDC grid.

B. Implementation

The implementation of the suggested controller has been done in Python using standard functions. The MTDC grid has been implemented in PowerFactory to be able to use the software MTDC power flow function, which provides the required measurements (currents, voltages and powers). The Python interface of PowerFactory allows to collect the measurements to initialize the MPC scheme. Once the controller finds a solution, i.e. the new converter setpoints, it is provided to PowerFactory in order to calculate the new power flow. Given the relatively slow response time of the proposed scheme, sequential static load flows are considered sufficient to capture the behaviour of the controller.

IV. RESULTS AND DISCUSSION

A. Results for balanced operation

The capabilities of the proposed control scheme are first demonstrated in a balanced system. This simulation case considers the change of power and average voltage references of the supervisory control.

Following market agreements, forecasted RES production or other relevant information, the AC-DC grid control provides the supervisory MTDC control with hourly (or mid-hourly, etc.) power schedules. Additionally, the average voltage reference setpoint of the MTDC can be modified in order to optimize the losses on the DC network as discussed in [6]. From those received references, the MTDC grid supervisory controller calculates the necessary actions to steer the system to the desired reference schedule.

Fig. 3 illustrates the active power flow per terminal in such a situation. The power and average DC voltage references of the supervisory controller are changed at $t = 15$ s of the

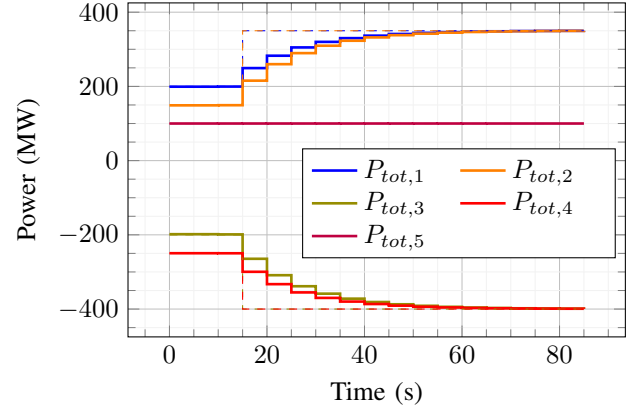


Fig. 3. Active power transfer per terminal. The dashed lines represent the reference power of each terminal

simulation. The DC voltages and their average at each time step is shown in Fig. 4. This validates the correct behaviour of the MPC, which is able to steer both the active power flows and the average DC voltage of the network to their respective reference values. Furthermore, the settling time of 40 seconds discussed in section II-D is hereby verified for a sampling time of 5 seconds and a control horizon of $N_c = 3$.

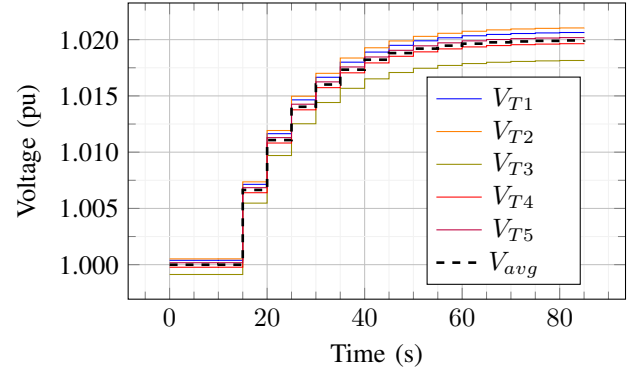


Fig. 4. Pole-to-neutral voltages in normal operation

B. Results for unbalanced operation

Following the outage of a single pole of a VSC terminal, the MPC should automatically redispatch the power flow through the MTDC grid between the positive and negative poles. This has to be done in a way that minimizes the deviation from the power schedule as much as possible while ensuring non-violation of the system various constraints. To illustrate this situation, the results of two simulation cases are presented. The first case considers an unconstrained neutral DC voltage while the second one imposes strict neutral DC voltage limits.

1) *Case of unconstrained neutral voltage:* In the case of unconstrained neutral DC voltage, the latter can vary freely depending on the unbalanced operation of the MTDC grid. In the simulation, the positive pole of terminal T3 is tripped at $t = 10$ s. Immediately after fault, all remaining dispatchable VSCs make up for the power loss through the implemented droop control. After this initial response of the system, the MPC calculates the set of actions to be taken to restore the power flow of the terminals to pre-fault levels (Fig. 5).

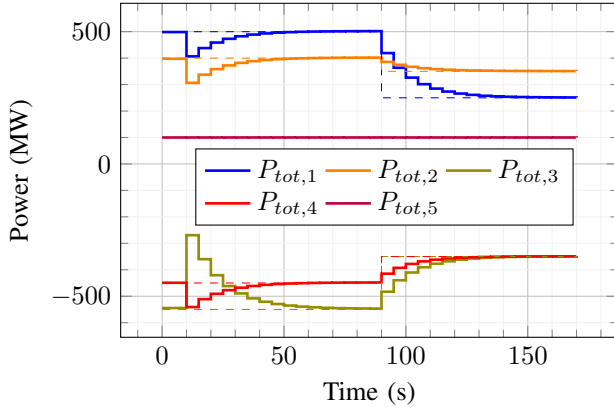


Fig. 5. Active power per terminal after trip of positive pole of T3

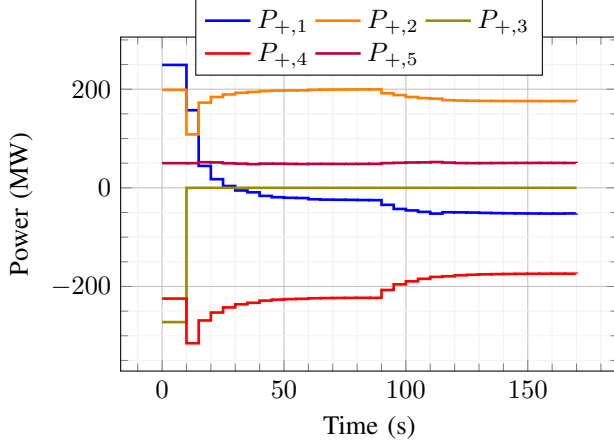


Fig. 6. Active power of positive pole after trip of positive pole of T3

Obviously, the power split between the two poles is uneven, as shown in Fig. 6 and Fig. 7.

The average voltages of the positive and negative poles, shown in Fig. 8, are impacted differently by this outage. On the affected pole, the excess active power on the MTDC grid leads to an increased average voltage. The controller steers the average voltage back to its reference value of 1 pu. At $t = 90$ s, a new average voltage setpoint of 1.02 pu is received, and the controller successfully brings all voltages around this new

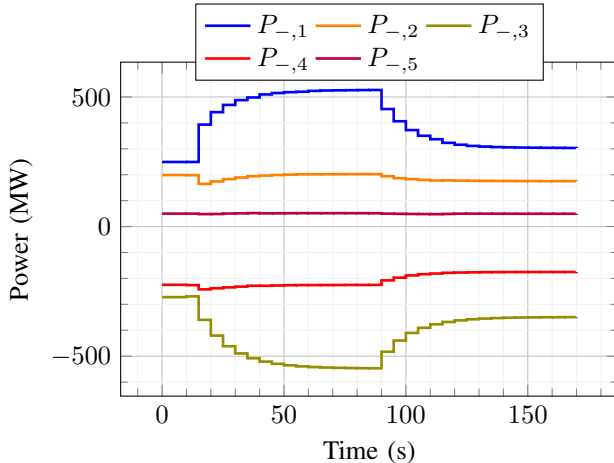


Fig. 7. Active power of negative pole after trip of positive pole of T3

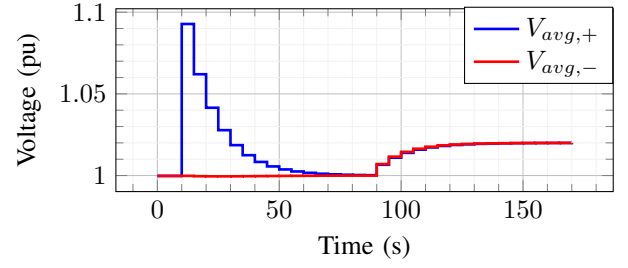


Fig. 8. Average DC voltages after trip of positive pole of T3

setpoint, even with the loss of one terminal pole.

2) *Case of constrained neutral voltage:* To illustrate the capabilities of the controller to constrain the neutral DC voltage, the same scenario as for the unconstrained case is simulated with a neutral DC voltage limited to ± 3.15 kV. This could correspond to an insulation limit on the DMR for example. As shown in Fig. 9, the MPC is able to keep this voltage above the corresponding limit, whereas the previous case led to a neutral DC voltage of -4.46 kV on terminal T3 (which is the most impacted).

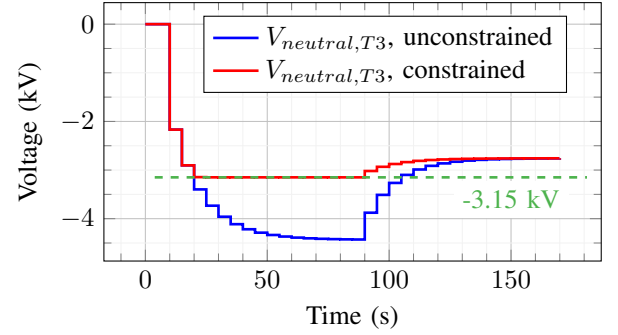


Fig. 9. Neutral DC voltage of terminal T3 for the constrained and unconstrained cases

This voltage regulation, however, is done at the expense of the desired power flow. In order to limit the neutral DC voltage, the controller has to reduce the power flow through the DMR as shown in Fig. 10. Here, the MPC receives new power setpoints at $t = 90$ s, which it is able to reach.

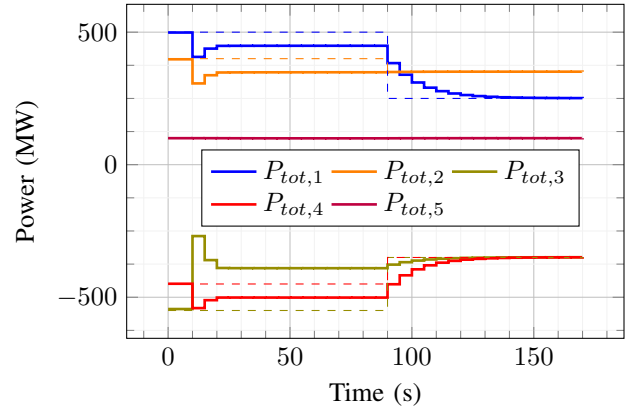


Fig. 10. Active power flow per terminal with neutral DC voltage limitation

V. CONCLUSION

This paper has proposed a supervisory control of an MDTC grid with bipolar configuration, inspired by MPC. It calculates a set of control actions required to smoothly steer the MTDC grid from one operating point to the desired one, while respecting various system constraints. It has been verified that such a supervisory controller is able to operate the MTDC within system limits both during normal operation and following outages, such as the trip of a pole, which leads to unbalanced operation of the DC network.

This unbalanced condition leads to current flowing through the DMR, leading to non-zero neutral DC voltage. In order to ensure safe operation, the DMR cable voltage limitations have to be respected. Thanks to the MPC formulation, this can be implemented as constraint in the optimization. As a result the supervisory controller can limit the neutral DC voltages and the current in the DMR, which may come at the expense of deviating from the desired power flow references.

REFERENCES

- [1] P. Rault. Dynamic Modeling and Control of Multi-Terminal HVDC Grids. PhD thesis, Ecole Centrale de Lille, L2EP, 2014.
- [2] D. Van Hertem and M. Ghandhari. Multi-terminal VSC HVDC for the European supergrid: Obstacles. *Renewable and Sustainable Energy Reviews*, 14(9):3156– 3163, dec 2010.
- [3] CENELEC, CLC/TS 50654-1:2020 : HVDC Grid Systems and connected Converter Stations - Guideline and Parameter Lists for Functional Specifications - Part 1: Guidelines, CENELEC, 2020.
- [4] T. K. Vrana, “System Design and Balancing Control of the North Sea Super Grid,” NTNU, 2013.
- [5] F. Thams, S. Chatzivasileiadis, E. Prieto-Araujo and R. Eriksson, “Disturbance attenuation of DC voltage droop control structures in a multi-terminal HVDC grid,” in *IEEE Manchester PowerTech*, 2017.
- [6] L. Papangelis, “Local and centralized control of multi-terminal DC grids for secure operation of combined AC/DC systems,” Univ. of Liege, 2018.
- [7] L. Papangelis, M.-S. Debry, P. Panciatici and T. Van Cutsem, “Coordinated supervisory control of multi-terminal HVDC grids: A model predictive control approach,” *IEEE Trans. on Power Systems*, 2017.
- [8] J. M. Maciejowski, *Predictive control: with constraint*, Pearson education, 2002.
- [9] S. J. Qin and T. A. Badgwell, “A survey of industrial model predictive control technology”, *Control Eng. Practi*, pp. 733-764, 2003.